Electronic Supplementary Material (ESI) for Chemical Communications.

Electronic Supplementary Information

Poly(amidoamine) nanoparticles cross-linked two-dimensional metal-organic framework nanosheet membrane for water purification

Yuan Peng,[a] Rui Yao [a,b] and Weishen Yang *,[a]

[a]*State Key Laboratory of Catalysis, Dalian Institute of Chemical Physics, Chinese Academy of Sciences, Dalian 116023, P. R. China*
[b]*University of Chinese Academy of Sciences, Beijing 100049, P. R. China*

Experimental Procedures

Materials

Hexahydrate zinc nitrate [$Zn(NO_3)_2 \cdot 6H_2O$, 99%] and benzimidazole (Bim, 98%) were purchased from Sigma-Aldrich. *N*,*N*-dimethylformamide (DMF, AR), methanol (AR) and n-propanol (AR) were purchased from Sinopharm Chemical Reagent Co.. PAMAM dendrimers (Generation 0 solution, ethylenediamine core, 20 wt. % in methanol; generation 4.0 solution, ethylenediamine core, 10 wt. % in methanol; generation 6 solution, ethylenediamine core, 5 wt. % in methanol) were purchased from Sigma-Aldrich. Evans blue was purchased from Sigma-Aldrich. Gold nanoparticles (5 nm, 0.01%w/v) were purchased from Shanghai Yuanye Biotechnology Co. Ltd. All the chemicals were used without further purification.

Synthesis of $Zn_2(Bim)_3$ precursors

Layered $Zn_2(Bim)_3$ precursors were prepared according to the following protocol reported by us previously.[1] A solid mixture of $Zn(NO_3)_2 \cdot 6H_2O$ and benzimidazole was dissolved in DMF under ultrasonic treatment with a molar ratio of Zn^{2+}/Bim/DMF = 1:0.5:130. After complete dissolution, the reaction solution was transferred to a Teflon-lined stainless-steel autoclave and kept at 100 °C for 72 h. The obtained product was isolated by filtration and washed thoroughly with methanol, and dried at 50 °C overnight in an air dry oven.

Exfoliation of layered $Zn_2(Bim)_3$ precursor into nanosheets

Before exfoliation, the pristine precursors were dried at 150 °C under vacuum for 24 h to remove the residual solvent and water adsorbed within the layers. $Zn_2(Bim)_3$ nanosheets were fabricated via a recipe according to our previous report.[1] Typically, 0.025 g $Zn_2(Bim)_3$ precursors were dispersed in a mixed solvent of methanol and n-propanol, 50 mL respectively, and transferred into a 150 mL ball milling jar equipped with 2 big iron milling balls with a diameter of 15 mm and 6 small balls with a diameter of 12 mm. The mixture was milled at a speed of 60 rpm for 70 min (PM400, Retsch Co.). Note that the jar rotated for 1 min and stopped for 15 s to impel the sedimentation of $Zn_2(Bim)_3$ particles, and then counter-rotated for another 1 min. The obtained nanosheet suspension was diluted 2.5 times with the same solvent mixture, then further exfoliation was performed by treating the suspension in an ultrasonic circulating water bath (600 watts, Branson, Emerson Co.) for 30 min at room temperature. Consequently, a colloidal suspension of $Zn_2(Bim)_3$ nanosheets was obtained after the sedimentation of large unexfoliated particles for at least two weeks. The concentration of nanosheets suspension was about 0.05 mg/mL.

Preparation of D-NS and D-NS membranes

Asymmetric α-Al_2O_3 disks (Inocermic GmbH) composed with two layers of alumina particles in different sizes were used as substrates in this study. The average pore size of the top layer is about 200 nm. The pretreatment of these porous supports was the same as

we have mentioned before.[2] Different generations of PAMAM dendrimer solutions were firstly diluted to the same molar concentration using methanol, *i.e.* 0.00072 wt. % for G0 solution, 0.02 wt. % for G4 solution, 0.08 wt. % for G6 solution. A certain amount of PAMAM solution was added into $Zn_2(Bim)_3$ nanosheets suspension with different volumes in accordance with different PAMAM loadings. As the PAMAM solution volume used for the membrane preparation was too small, therefore the NS suspension volume practically equaled to that of the D-NS suspension. The mixture was treated in an ultrasonic bath for 5 min at room temperature to allow "one-step self-assembly" between the PAMAM and the NSs,[3] The obtained D-NS complex was washed with methanol and used for various characterizations.

Porous substrate was placed in a home-made filtration setup. A certain volume of D-NS suspension based on the membrane thickness was vacuum-filtrated through the sealed substrate at room temperature. During this process, the vacuum degree was maintained at approximately 0.012~0.014 MPa for the sake of preventing the flexible NSs from being sucked into the substrate pores. After the suspension was filtrated thoroughly, 5 mL methanol was subsequently filtrated through the obtained membrane in order to take away redundant PAMAM particles that did not graft on the NSs. The as-synthesized membranes were kept in the setup until the pressure was restored to atmospheric condition. No drying procedures were required afterward.

Characterizations

X-ray diffraction (XRD) measurements were performed on Rigaku D/MAX 2500/PC (λ=0.154 nm at 40 kV and 200 mA). The data were recorded with a scan speed of 5 °/min. Scanning electron microscopy (SEM) images were obtained on a Quanta 200 FEG instrument (FEI Co.). To improve the electrical conductivity of the samples, they were sputtered with gold for 60 s before characterization. For the cross-section imaging, the membranes were broken and adhered to the side face of a cubic metal block. Atom Force Microscopy (AFM) images were recorded with a MultiMode 3D AFM (Bruker Co.) operated in tapping mode. The D-NS suspension was dropped on silica wafer and dried at room temperature, and then was observed under tapping mode. All the images were recorded using 0.01-0.025 Ohm-cm Antimony (n) doped Si cantilevers (RTESPA-300, Bruker Co.). The spring constant was 40 N/m and the resonant frequencies were 300 kHz. Infrared spectra were recorded on a Nicolet 6700 Fourier Transform Infrared Spectroscopy-Attenuated Total Reflectance (FTIR-ATR, Thermo Scientific Co.) spectrophotometer. The spectra backgrounds were recorded 32 times, and then, the spectra of the samples were recorded 32 times. X-ray photoelectron spectroscopy (XPS) characterization was utilized to collect the surface elements information of the pure MOF NS membrane and the D-NS membrane dried at 120 °C under vacuum for 12 hours, and it was performed on a thermos ESCALAB 250Xi X-ray photoelectron spectrometer equipped with a monochromatic Al Kα X-ray source. The ultraviolet –visible (UV/Vis) absorbance

spectra were collected on Shimadzu UV-2600 spectroscopy.

Water purification tests of the pure NS membrane and the D-NS membranes

The obtained membranes were sealed in a home-made dead-end filtration apparatus. The membrane edge was covered with silicone rubber pads and stainless-steel gaskets with a hole of 10 mm in diameter in the center to prevent scratches on the membranes from O-rings. The effective membrane area was 0.785 cm^2. The membranes underwent a water compaction process firstly at 5 bar for 1 hour, the pure water permeation reached an equilibrium state after about 30 min. And then water purification tests were conducted at 1 bar for 1 hour. Evans blue aqueous solution (10 μmol/L) and gold nanoparticle aqueous solution (10^{11}/mL) were used as the feed solution for the separation performance evaluation. The concentration of feed solution and permeate solution were measured by UV/Vis spectroscopy. To eliminate concentration polarization in the feed side since the feed concentration gradually increased as the water molecules transported through the membranes to the permeate side, the volume of feed solution was constant at 500 mL. The rejection rate (*R*) was calculated by the following equation:

$$R\ (\%) = \frac{C_0 - C}{C_0} \times 100\%$$

Where C_0 and C are the solution concentration in the feed side and the permeate side, respectively.

The water flux (*F*) was calculated by the following equation:

$$F = \frac{V}{At\Delta P}$$

Where V (L) is the volume of permeate solution collected over a period of time (*t*, h), A is the effective membrane area (m^2), and ΔP is the transmembrane pressure difference (bar).

Results and Discussion

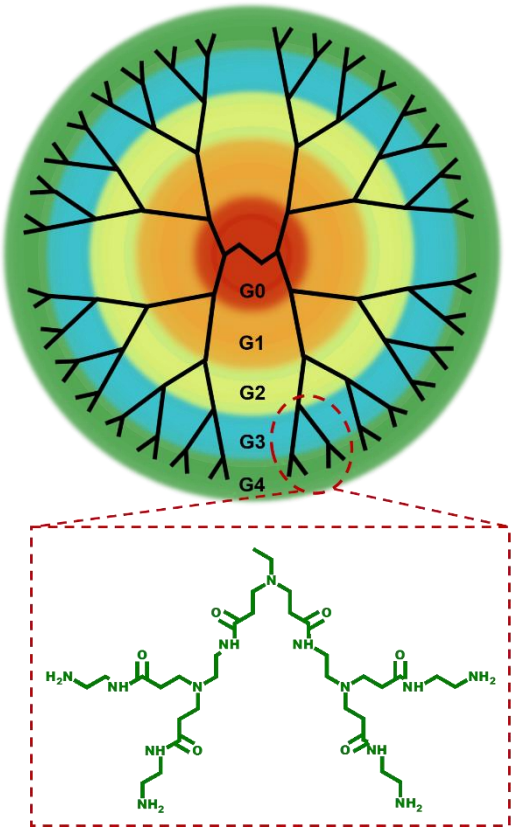

Figure S1. The structure of PAMAM G4. Rings with different colours represent the extra repeat functional units compared with the previous generation.

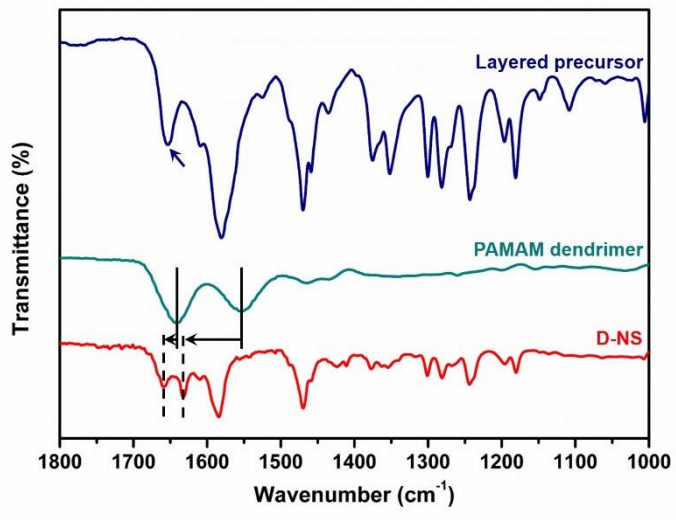

Figure S2. FTIR spectra of the layered $Zn_2(Bim)_3(OH)(H_2O)$ precursor, the PAMAM dendrimer and the D-NS complex.

For the layered precursor, the peak at 1653 cm^{-1} was an indication of -C(O)N- stretching vibration assigned to DMF molecules that detained between the sheets of the layered precursors. Correspondingly, the vibration was masked by the strong amide I mode vibration of PAMAM particles in the spectra of the D-NS, since the DMF amount in the D-NS nanosheet suspension used for membrane fabrication was much less than that within the precursors.

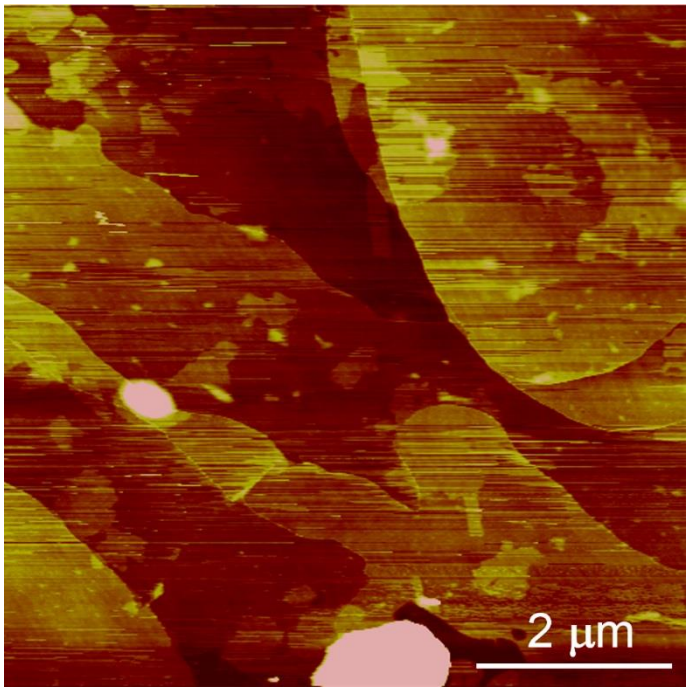

Figure S3. AFM image of the pristine NSs.

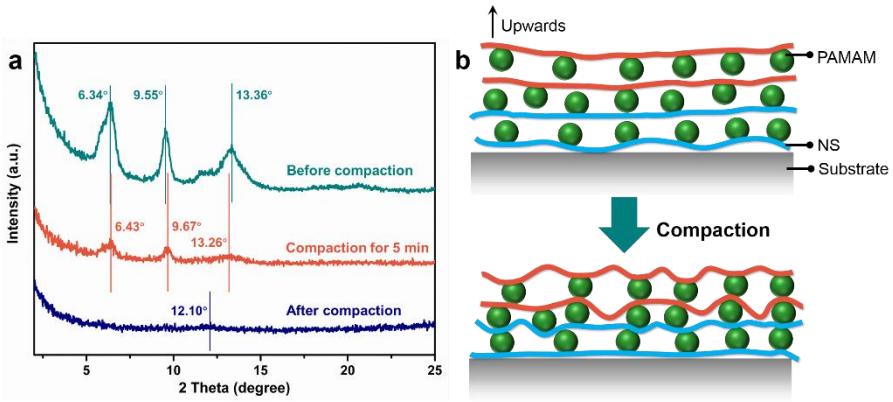

Figure S4. a) The XRD patterns of D-NS membrane before and after the pure water compaction procedure at 5 bar. b) Illustration of the membrane structure evolvement during the water compaction process.

As the compaction process went on, the first two characteristic peaks at 6.3° and 9.6°, respectively, shifted to higher 2Θ values, which were assigned to the PAMAM grafting area within D-NS membrane, the interlayer spacing became constrictive under high compaction pressure, and these two peaks disappeared ultimately owing to the PAMAM random arrangement of PAMAM on the NSs. While the peak at 13.4° was assigned to the remaining non-grafting NS area. The water molecules constrained between the adjacent NSs would swell the interlayer spacing when the pressure returned to the atmospheric state, leading to an expanded interlayer spacing. The results once again exemplified the cross-linking effect of PAMAM within the D-NS membranes.

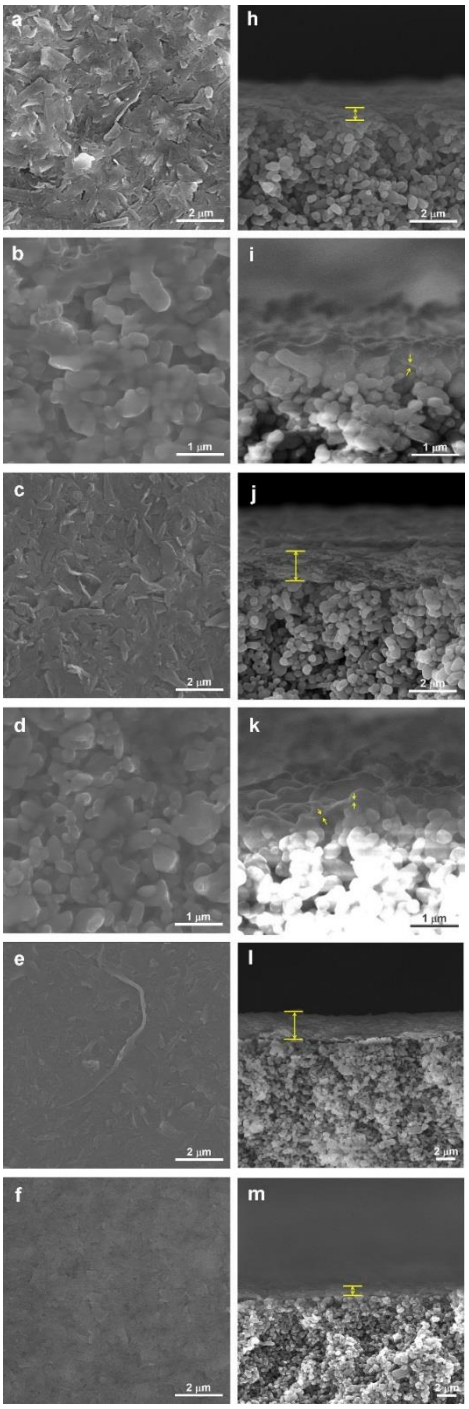

Figure S5. Top view of the as-synthesized D-NS membranes using a) 15mL, c) 40 mL, e) 80 mL NS suspension, and the corresponding membranes using b) 15 mL, d) 40 mL, f) 80 mL NS suspension after water compaction procedure. h-m) Cross-section view of these membranes corresponding to the left column.

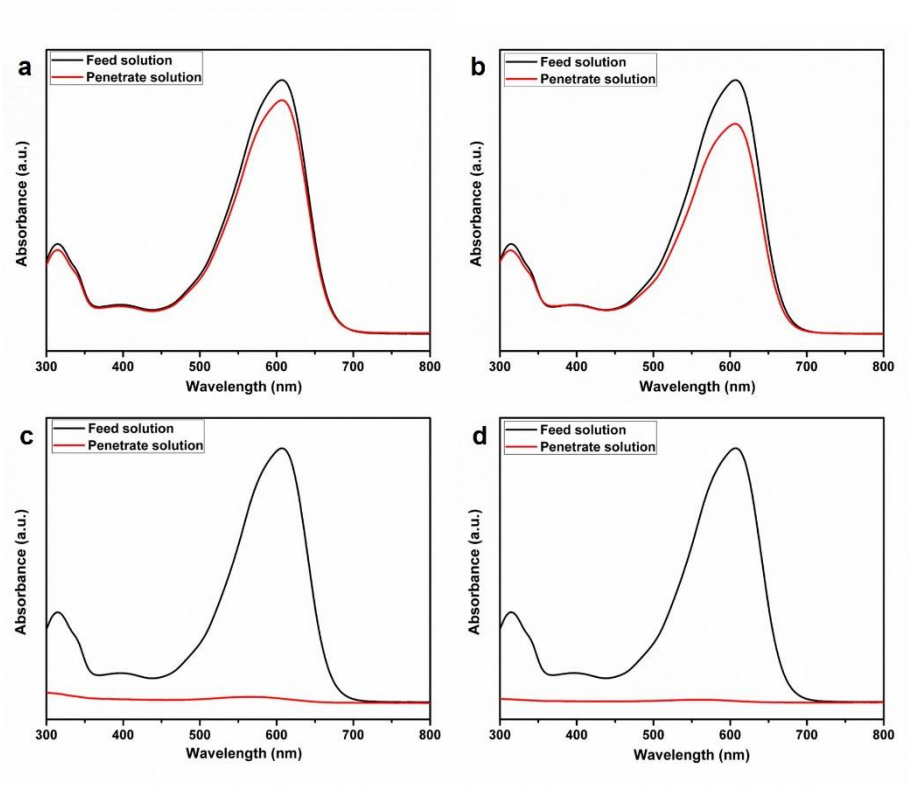

Figure S6. UV/Vis spectra of the EB feed solution and the permeate solution collected using the D-NS membranes prepared with a) 15 mL, b) 40 mL, c) 60 mL, d) 80 mL D-NS suspension.

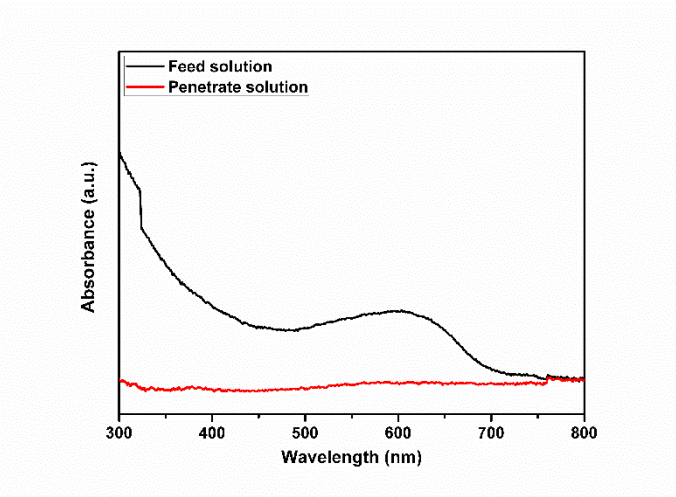

Figure S7. UV/Vis spectra of the Au feed solution and the permeate solution of D-NS membrane prepared with 15 mL D-NS suspension.

Obviously, for the filtration process of gold particle (5 nm in diameter) solution, the water flux of the D-NS membrane was high than that of the D-NS membrane used for EB separation. The size of the PAMAM G4 spacers was only 4.5 nm, and the interaction force between the adjacent NSs was much enhanced with the PAMAM grafted on. Therefore, gold particles larger than 4.5 nm could not permeate through the D-NS membranes. Instead, more water molecules would permeate through the interlayer galleries within the membranes, resulting in the increment of water flux compared to the EB molecule separation performance.

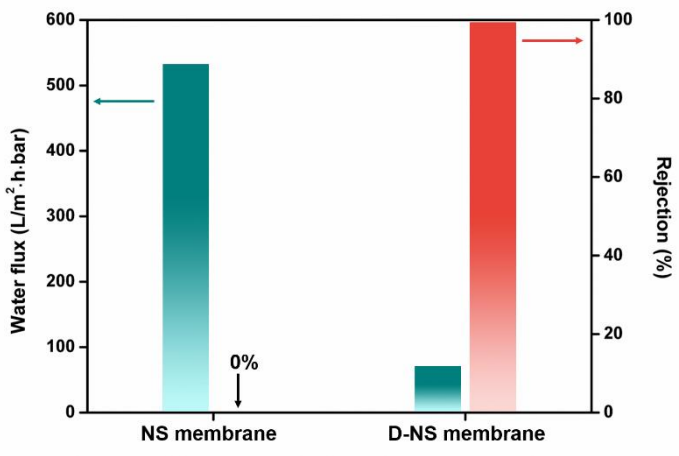

Figure S8. EB molecule separation performance of the pristine MOF NS membrane and the D-NS membrane.

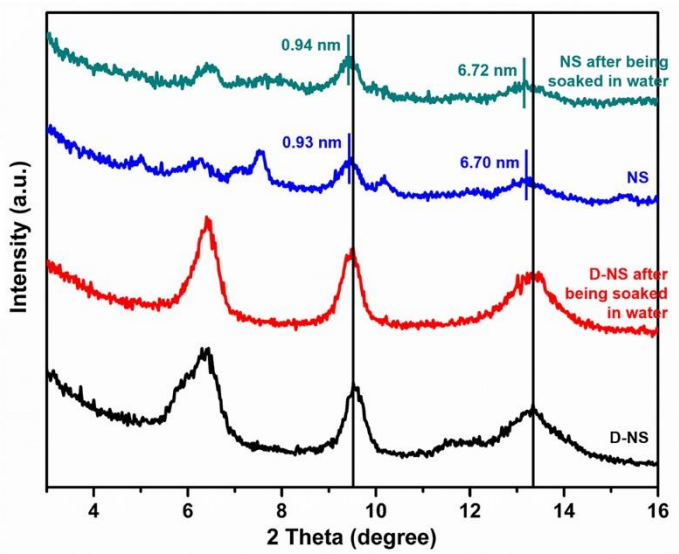

Figure S9. The XRD patterns of as-synthesized NS and D-NS membranes before and after immersion in water.

To evaluate the swelling degree in water, the as-synthesized NS and D-NS membranes were soaked in water for 40 min and were characterized by XRD for the structure and interlayer spacing changes. For the NS membrane, the peak at 5.2° and 10.3° which were assigned to the pristine layered precursor disappeared after immersion in water, we assumed it was ascribed to a severe swelling of the stacking nanosheet structure.[4] And the peak at 7.6° suggesting an expanded nanosheet stacking gradually developed into a wide hump, corresponding to a d-spacing of 1.14 nm. In addition, three peaks at $2\theta = 6.3°$, 9.6°, 13.4° all demonstrated a shift with some degree. While with PAMAM cross-linking, the XRD patterns of the D-NS membrane showed no changes, revealing a good anti-swelling capacity, and therefore a significantly improved dye rejection and a relatively low water flux compared with NS membrane.

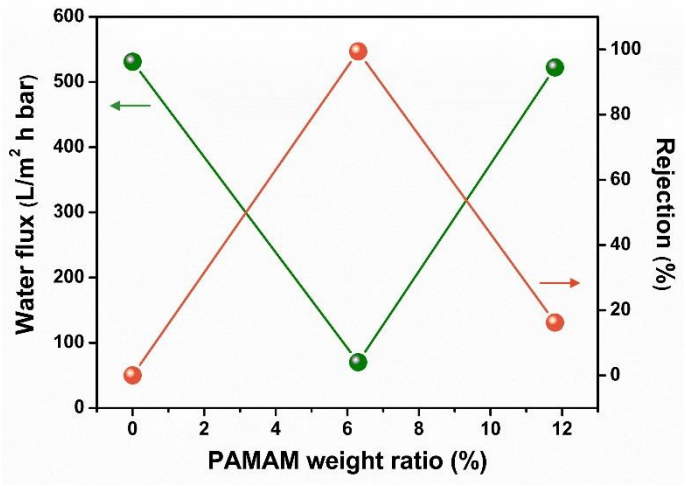

Figure S10. The effect of PAMAM loading on the D-NS membrane performance for the removal of EB molecules.

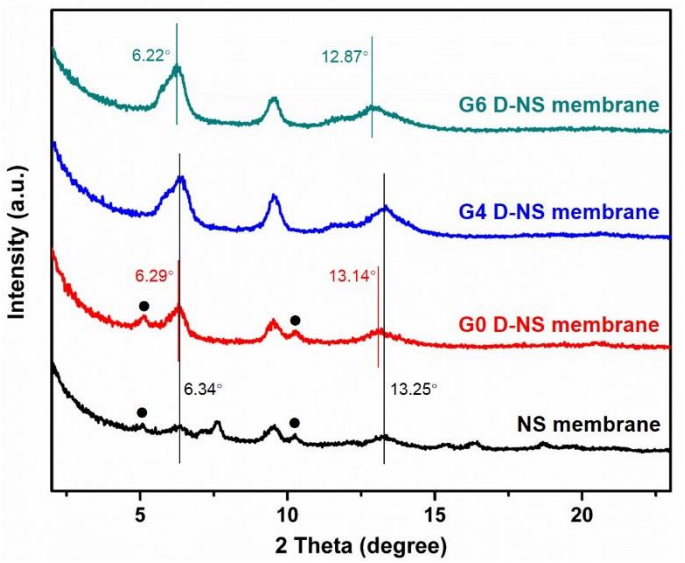

Figure S11. XRD patterns of D-NS membranes prepared using different generations of PAMAM dendrimers. The black dots represent the (001) and (002) reflection of layered $Zn_2(Bim)_3(OH)(H_2O)$ precursor.

Table S1. The properties of different generations of amino group-terminated PAMAM.

Generation	Molecular weight	Diameter (nm)	Terminal group amount
G0	517	1.5	4
G4	14215	4.5	64
G6	58048	6.7	256

Data from Dendritech, Inc.

Table S2. Comparison of separation performance with other functional membranes for dye removal applications.

Membrane	Dye molecule	Water flux (LMHB)	Rejection (%)	Ref.
COF-LZU1	Methyl blue	49	99.2	5
MoS_2	Evans blue	245	89	6
GO	Evans blue	63	87	7
g-C_3N_4	Evans blue	12	90	8
21%Ag@MXene	Methyl green	354	92.3	9
UiO-66-rGO	Rhodamine B	30.6	95	10
ZIF-8/PSS	Methyl blue	27	98.6	11
PA/ZIF-8(B)	Congo red	2.3	99.98	12
F127/PES	Alcian blue	18	95.7	13
D-NS	Evans blue	67	99.6	This work

References

[1] Y. Peng, Y. S. Li, Y. J. Ban, W. S. Yang, *Angew. Chem. Int. Ed.* **2017**, *56*, 9757-9761; *Angew. Chem.* **2017**, *129*, 9889-9893.

[2] Y. Peng, Y. S. Li, Y. J. Ban, H. Jin, W. M. Jiao, X. L. Liu, W. S. Yang, *Science* **2014**, *346*, 1356-1359.

[3] Y. Z. Piao, T. F. Wu, B. Q. Chen, *Ind. Eng. Chem. Res.* **2016**, *55*, 6113-6121.

[4] K. Nakagawa, S. Araya, M. Kunimatsu, T. Yoshioka, T. Shintani, E. Kamio, H. Matsuyama, *Membranes*, **2018**, *8*, DOI: 10.3390/membranes8040130.

[5] H. W. Fan, J. H. Gu, H. Meng, A. Knebel, J. Caro, *Angew. Chem. Int. Ed.* **2018**, *57*, 4083-4087; *Angew. Chem.* **2018**, *130*, 4147-4151.

[6] L. W. Sun, H. B. Huang, X. S. Peng, *Chem. Commun.* **2013**, *49*, 10718-10720.

[7] H. Huang, Y. Mao, Y. Ying, Y. Liu, L. Sun, X. Peng, *Chem. Commun.* **2013**, *49*, 5963-5965.

[8] Y. J. Wang, L. B. Li, Y. Y. Wei, J. Xue, H. Chen, L. Ding, J. Caro, H. H. Wang, Angew. *Chem. Int. Ed.* **2017**, *56*, 8974-8980; *Angew. Chem.* **2017**, *31*, 9102-9108.

[9] R. P. Pandey, K. Rasool, V. E. Madhavan, B. Aïssa, Y. Gogotsi, K. A. Mahmoud, *J. Mater. Chem. A* **2018**, *6*, 3522-3533.

[10] K. C. Guan, D. Zhao, M. C. Zhang, J. Shen, G. Y. Zhou, G. P. Liu, W. Q. Jin, *J. Membr. Sci.* **2017**, *542*, 41-51.

[11] R. Zhang, S. L. Ji, N. X. Wang, L. Wang, G. J. Zhang, J. R. Li, Angew. *Chem. Int. Ed.* **2014**, *53*, 9775-9779; *Angew. Chem.* **2014**, *126*, 9933-9937.

[12] L. Y. Wang, M. Q. Fang, J. Liu, J. He, L. H. Deng, J. D. Li, J. D. Lei, *RSC Adv.* **2015**, *5*, 50942-50954.

[13] Y. Zhang, Y. L. Su, W. J. Chen, J. M. Peng, Y. N. Dong, Z. Y. Jiang, *Ind. Eng. Chem. Res.* **2011**, *50*, 4678-4685.

[12] Y. Zhang, Y. L. Su, W. J. Chen, J. M. Peng, Y. N. Dong, Z. Y. Jiang, *Ind. Eng. Chem. Res.* **2011**, *50*, 4678-4685.